LAWRENCE
LIVERMORE
NATIONAL
LABORATORY

LLNL-CONF-670643

R&D Effort for ITER Central Solenoid

N. N. Martovetsky, D. K. Irick, R. P. Reed, W. T. Reiersen, J. P. Smith

May 13, 2015

Symposium on Fusion Energy
Austin, TX, United States
May 31, 2015 through June 4, 2015

Disclaimer

R&D Effort for ITER Central Solenoid

Nicolai N. Martovetsky
US ITER,
LLNL/ORNL
Oak Ridge, TN, United States
nmk@ornl.gov

David K. Irick
Department of Mechanical, Aerospace, and Biomedical Engineering
University of Tennessee Knoxville
Knoxville, TN, United States
dki@utk.edu

Richard P. Reed
Cryogenic Materials Inc.
Boulder, CO, United States,
rpreed@comcast.net

Wayne T. Reiersen
US ITER,
PPPL
Oak Ridge, TN, United States
wrn@ornl.gov

John P. Smith
General Atomics
San Diego, CA, United States,
John.Smith@ga.com

***Abstract*—The US ITER organization is responsible for supply of the Central Solenoid (CS) to the ITER collaboration. This 1,000 t object is the largest pulsed superconducting magnet ever built.**

Research and development on the CS began in 2007, long before the CS Module Fabrication (CSMF) subcontractor was selected, to develop validated design options early in the process and minimize schedule impacts. General Atomics (GA) was awarded the CSM fabrication contract in 2011. Technology developed before then was transferred to GA, which then began its manufacturing development program. This paper reports on the R&D work carried out by the US ITER Project Office and GA to support fabrication efforts.

The R&D effort can be divided into the following major categories: (1) fabrication feasibility studies; (2) development and qualification of the performance of the critical components (joints, inlets, insulation, etc.); and (3) characterization of the CS materials. This paper gives an outlook of the R&D effort and main results by the US team for CS in the following areas: (1) winding; (2) joint development; (3) welding development and qualification; (4) inlets and outlets development; (5) heat treatment; (6) insulation development; and (7) vacuum pressure impregnation.

Keywords—superconducting magnets, welding qualification, heat treatment, fabrication

I. Introduction

The Central Solenoid (CS) will be built by US ITER and supplied to the ITER machine. Fabrication of the CS requires many critical steps, most of which were not completely established in previous projects. The most relevant magnet, ITER Central Solenoid Model Coil (CSMC) was built by a United States–Japan collaboration and tested in 2000 [1]. This experience was very valuable in CS research and development (R&D); however, the ITER CS had many features that needed to be developed from scratch. In the beginning of the project, we concentrated mostly on feasibility issues rather than on optimization of fabrication, which is vendor dependent.

II. Winding

A. Preliminary trials

Preliminary winding exercises were performed to determine the evolution of the conductor behavior during conductor spooling, straightening, and forming of the coil that reflected the manufacturing process. Fig. 1 shows the first trials of the conductor forming and assembly on the winding table.

Reproducibility of the bending, twisting, and keystoning, forces to keep the turns in the desired position was the focus of the studies. This information was necessary for the winding tool development but also for a definition of realistic tolerances in the winding pack, turn-to-turn, and layer-to-layer spacing in the winding pack.

Fig. 1. First winding trials and assembly of the pancake on the winding table.

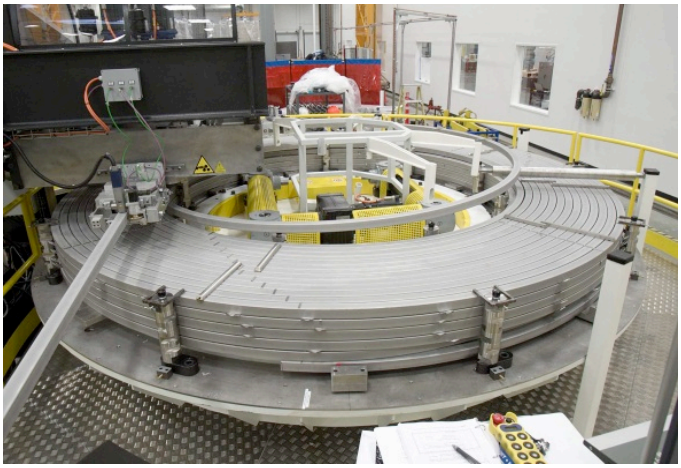

Fig. 2. Winding table at GA.

B. Development of the production winding system

General Atomics (GA), our industrial partner, developed a highly automated winding system that included the following components: (1) de-spooling; (2) rough and fine straightening; (3) grit blasting; (4) conductor washing; and (5) automated turns forming, including radial transitions, fixing the space between the turns, and location of the turns relative to each other. The system keeps track of the turn length during the winding process and allows for an efficient winding process. The system was commissioned at the factory and then at the fabrication site. The system was qualified on the mockup fabrication. The winding table with the wound hexapancake is shown in Fig. 2.

III. Develoment of the joints

Three types of joints are employed in the CS [2], as shown in Fig. 3. Interpancake joints (42 total) connect the seven conductors that constitute the CS module. The joints that attach the CS module (CSM) terminations to the bus extensions (12 total) are soldered to provide a possibility to undo and redo the joints for module disassembly, if necessary. The third type of joints is used for connections to the feeders (12 total). This type of joint, called twin box was developed and used in the Toroidal Field Model Coil [3]. For CSM, we modified dimensions and optimized the manufacturability of the joint box.

The interpancake joint is a sintered one. The joint is assembled and closed in the envelope of the regular conductor cross section, and the joint forms and sinters during the reaction heat treatment. It is assembled from six subcables from each side and, therefore, is called "6 × 6." Half of the subcables of the next-to-last stage are cut and reassembled so that the finished joint will not be thicker than the cable. The sintered joint is compacted to approximately 20% of the void fraction in the cable space. It has helium in the cable space and in a central channel all the way through the joint. A schematic of the sintered joint is shown in Fig. 4. The coaxial joint between the termination and the bus is shown schematically in Fig. 5.

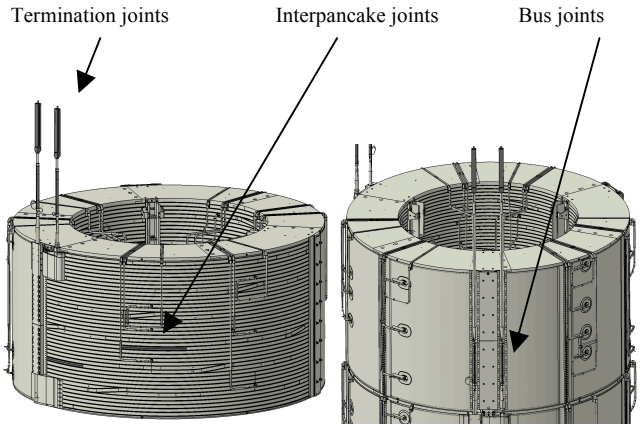

Fig. 3. Types of joints in the CS.

Six sintered joints were built and tested in the R&D effort. We checked the sintering and the aging issue for the interpancake joints to avoid any surprises with exposure of the joint to atmospheric air during several months from assembly of the joint to heat treatment (HT) of the coil. The testing took place with currents up to 80 kA. The scatter of the resistance was remarkably low; all of the joints showed 0.12–0.14 nOhm at above 40 kA, which is well within the specified limit of 4 nOhm.

The key element of the bus joint is the laced cylinder (union) that has a double layer of the superconducting strands, which are soldered to the copper tube. The cross section of the joint is shown in Fig. 6, where soldered and sintered interfaces can be seen.

There are two soldering processes: one uses a Sn-5%Sb solder that holds the superconducting strands, whereas the second soldering process is used to complete the assembly of the joint with the Pb%40-Sn solder. Higher melting temperature of the solder in the first process allows the second soldering without disturbing the laced union.

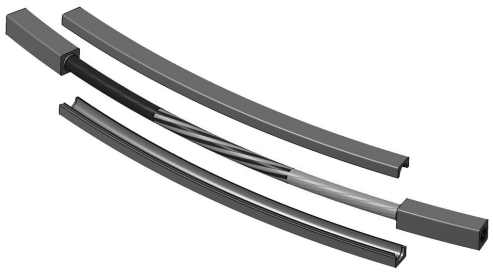

Fig. 4. Sintered interpancake joint for CSM

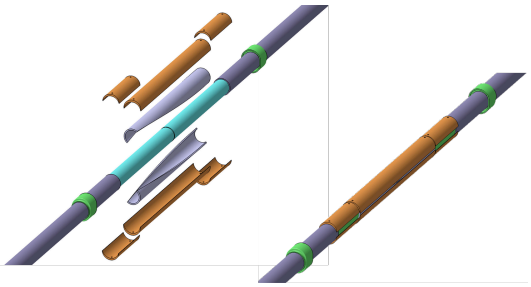

Fig. 5. Bus joint in CS—exploded view (left) and the assembly (right) before welding the close out case.

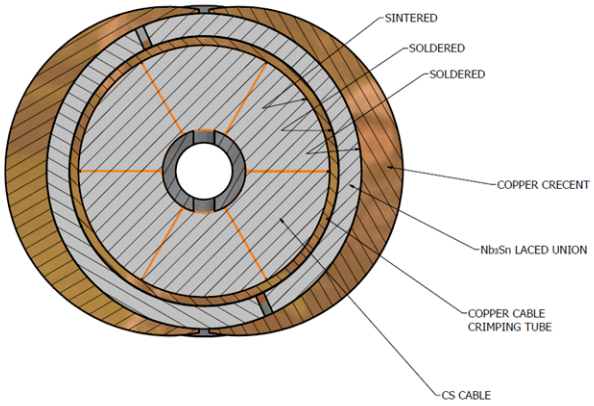

Fig. 6. Cross section of the bus joint.

A. *Joint testing facility and joints qualification*

To test the joints developed for the CSM, we built a Joint Testing Apparatus [4]. The schematics of the apparatus and its realization are shown in Fig. 7.

The principle of the apparatus is a superconducting transformer. The primary coil inside is wound out of more than 1,000 turns of the NbTi wire with an operating current of 200 A. The secondary coil is a one-turn racetrack that contains one or two joints in the turn. The sintered joint racetracks had one joint, and the bus joint racetracks had two joints due to complexity of the assembly. When the current is introduced into the primary coil, it induces a large current; up to 50 kA in the secondary coil containing the joint. When the current in the primary coil is held constant, the current in the secondary racetrack decays in accordance with the constant time, which is L/R_{joint}. Knowing the inductance of the racetrack, we can determine the joint resistance. The apparatus is equipped by two Hall probes that are located as shown in Fig. 7; their positions are known precisely. These Hall probes allow detection of not only the decay time, but also the absolute current in the secondary coil [4]. In addition, resistances of the joints were measured by direct measurement of the voltage across the joint by a digital microvoltmeter. During joint development, we tested 10 racetracks with four different types of joints, including two accepted for the CSM and two rejected (butt joints and 3×3 sintered joints; see [4] for details), despite the fact that all met the resistance requirements except the 3×3 sintered joint.

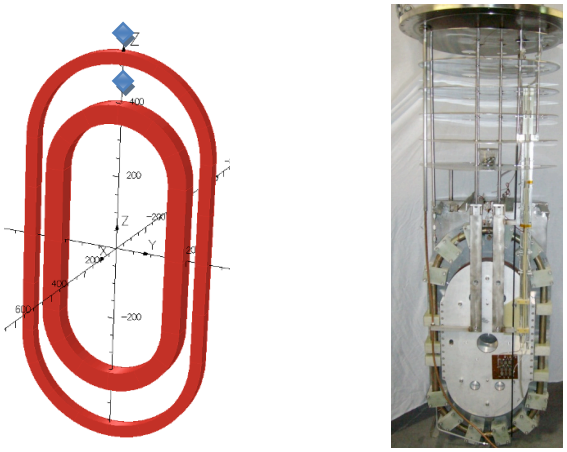

Fig. 7. Left, principle of the joint testing apparatus (diamonds show location of the Hall probes) and right, completed assembly before lowering into a cryostat.

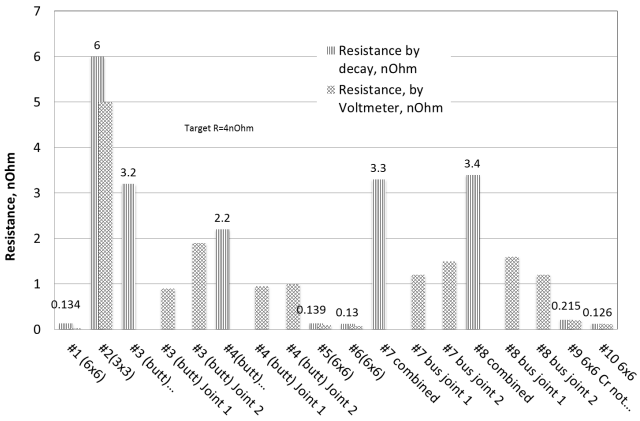

Fig. 8. Summary of the CS joint resistance measurements

IV. Welding Development and Qualification

The CS module has several welded joints. Helium inlet bosses are welded to the jacket at the inner diameter. All other welded joints are located at the outer diameter: closeout welds around joints and joints around breakouts, where the conductor separates from the winding pack and runs along the module, as shown in Fig. 3.

Features of the welding development included non-standard material of the jacket, a limit on the cable temperature during welding, and a complete joint penetration requirement on all the welded joints. The filler material for all the joints—including 316LN to JK2LB and 316LN to 316LN—is JK2LN because of its superior fracture toughness properties after heat treatment.

Welding development by the US ITER Project Office (USIPO) before placing the contract with the industrial partner focused on the feasibility of the welds with full penetration and the possibility of limited, controlled overheating of the superconducting cable. Also, welds of the JK2LB to JK2LB (material of the conductor jacket) and JK2LB to 316 LN were

qualified in accordance with the American Society of Mechanical Engineers' Boiler and Pressure Vessel Code, section IX. All efforts were limited by manual welding. Because of this effort, design of the weld preparation and main welding parameters were established. Further development and qualification carried out by GA and its partners include developing production equipment (mostly for automated welding), establishing nondestructive evaluation (NDE) methods and procedures, and qualifying the welds and welders. This effort is scheduled for completion in the first half of 2015.

V. Development of the Helium Inlet

The CS inlet is located at the inner diameter (ID) of the CSM to inject the coldest helium into the area of the lowest current sharing temperature (Tcs) in the magnet. The inlet and the butt joint are the critical parts of the CS that determine the life of the CSM; therefore, the inlet deserves careful analysis and consideration. It is a high-risk fabrication item because machining and welding are taking place near the cable that can be damaged. The original design of the inlet proposed by the ITER conceptual design was analyzed from the standpoint of manufacturability, hydraulic properties, and mechanical properties, especially fatigue characteristics.

The alternative proposal developed by USIPO provides better hydraulic and mechanical properties and, from the fabrication standpoint, a far less risky and economical inlet, thus reducing risk of cable damage and cost of the inlet fabrication. The development effort and the final design justification are described in [5–6]. The boss is oval, and the welds will have a smooth transition to the conductor to reduce stress concentration in the conductor and the welds. An adequate NDE procedure will be developed to keep welding defects to a minimum. In addition, we plan to use ultrasonic peening to create a compressive strain in the area of maximum stress that should significantly improve the fatigue life of the inlet [7]. The final design of the inlet is shown in Fig. 9.

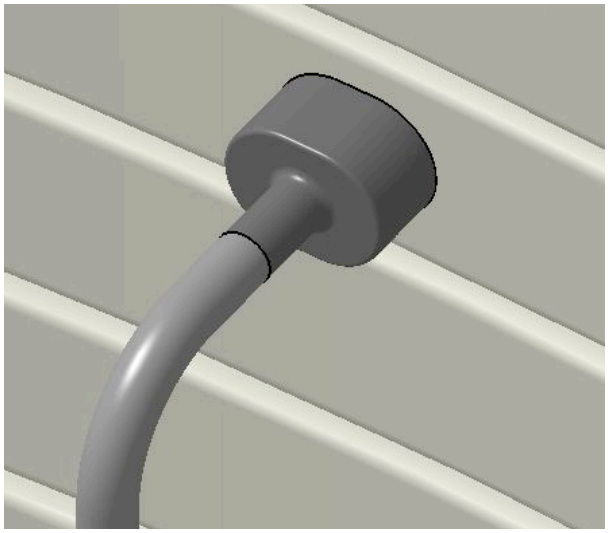

Fig. 9. CS inlet at the ID of the CS with the helium tube.

VI. Heat Treatment Studies

The Nb_3Sn superconductor is created during heat treatment of the conductor. A heat treatment schedule is proposed by the strand vendor within certain constraints by ITER but has no tolerances on the HT schedule (temperatures and durations). Exact implementation of the prescribed schedule is difficult in industrial conditions because of the high mass and thermal inertia of the CS and nonuniform temperature distribution across cross section of the winding pack. The original tolerance imposed on the HT schedule was very tight: +/-5°C, which is problematic or impossible to achieve for a big coil. We studied the heat treatment deviation effect on the final properties of the strand-current carrying capacity for several strands that will be used in the CSM. Fig. 10 shows results of a strand from JASTEC (one of the CS strand suppliers) that indicates heat treatment sensitivity to deviations from the optimum heat treatment schedule. A low sensitivity to these deviations from optimal parameters allowed for an increase in the tolerance band for the industrial heat treatment schedule and a significant reduction in the cost and the risk of the HT operation.

VII. Quench Detection System Development

The ITER CS magnet needs to be protected against overheating of the conductor in case of the occurrence of a normal zone (NZ). Because of a large amount of stored energy and slow NZ propagation, the NZ needs to be detected and the switchyard needs to open the breakers and send the current into the dump resistor within 2 s after detection of the NZ. The challenge is that we need to suppress the inductive voltage, which is 11 kV, across the module at the plasma initiation to

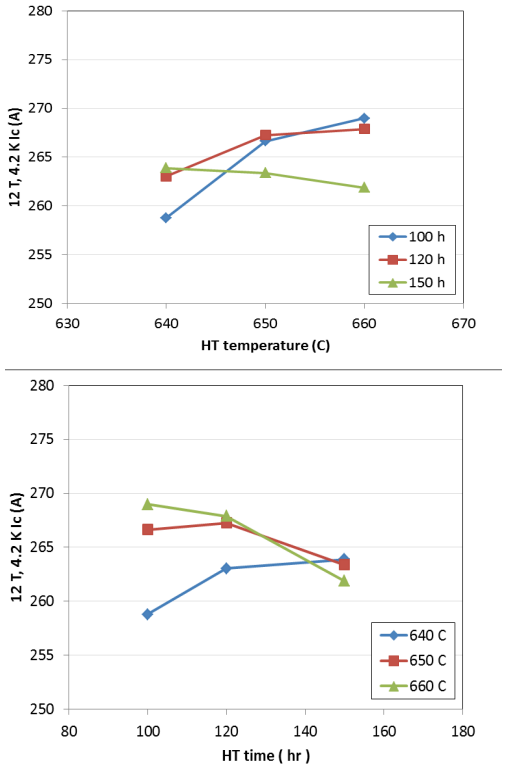

Fig. 10. Sensitivity of the critical current Ic (critical current) to temperature (upper plot) and duration (lower plot) of the heat treatment parameters

the level that we should be able to detect the resistive voltage of 0.3–0.5 V. Usual methods of quench detection are not even close to the CS requirements.

Two redundant schemes are proposed as the baseline for the CS quench detection (QD) System:

1) A scheme with Regular Voltage Taps (RVTs) from triads of Double Pancakes supplemented by Central Difference Averaging and by digital suppression of the inductive voltage from all active coils (the CS and PF coils). Voltage taps are taken from helium outlets at the CS outer diameter.

2) A scheme with the Cowound Voltage Taps (CVTs) taken from cowound wires routed from the helium inlet at the CS inner diameter.

For the cowound sensors, we developed a glass tape that contains two steel strips that serve as QD wires. The tape is wrapped around the conductor during turn insulation installation. A similar design was accepted by the TF system shortly after that. This design allows winding the tape around the conductor with a certain twist pitch to reduce the inductive noise in the CS and to provide the best possible coupling with the conductor. The CVT system will have the lowest noise signals, but it cannot be repaired, while RVT is repairable but has lower sensitivity.

A summary of results of the numerical modeling of the performance of both CS QD systems is presented in [8].

VIII. Insulation Development

Electrical insulation in high voltage magnets is one of the most responsible parts. Most magnet problems occur because of insulation failures. Insulation is not only a dielectric but also a structural member. Mechanical stress intensity in the conductor jacket is about 30% higher when the insulation does not provide a good support to the conductor. The following aspects of the insulation were addressed in the R&D phase:

- Dielectric strength of the turn insulation
- Mechanical properties of insulation
- Permeability of the insulation by the resin during vacuum pressure impregnation (VPI)
- Qualification of the special parts of insulation (breakout and inlets/outlets) and high voltage (HV) wire extraction from the CSM
- Development of the adequate VPI procedure for CSM

The dielectric strength of the insulation was tested on several mockups of turn insulation after cyclic tests at loads simulating stresses that the insulation will see in operation. We also built a mockup with the real turn and ground insulation in the full cross section 14 × 40 array and on two mockups with the inlet and ground insulation. Additionally, we built and tested a mockup of the helium tube simulating HV cable penetration underground insulation. The turn insulation could take up to 25–40 kV (highest in operation is 1,500 V); the ground insulation did not break down in the worst cases at 125–150 kV (highest fault is 29 kV). Thus, our design provided a sufficiently high safety margin, close to the design goal of a safety factor of 5 or higher. Below we give a brief description of some important steps in the insulation development.

A. *Qualification of the turn insulation*

Structural analysis of the winding pack showed that some areas of the winding pack, mostly in the corners of the conductors, could not meet structural design criteria. Mostly it is associated with a high coefficient of the thermal expansion (CTE) of the insulation through thickness and bending the walls of the conduit under the electromagnetic load that caused localized high tensile stress that was higher than the allowable values. That led us to qualification by testing. We chose a 4 × 4 array of conductors that were cyclically loaded in the compressive loads up to 90 MPa for 1.2 Mcycles at 80 K. That corresponds to 20 times cycling life in operation. Structural analysis showed that the loading in this condition closely resembles the distribution of the stress in the operating conditions of the winding pack. The total amount of the 4 × 4 arrays that were tested in the R&D effort was six [9–13].

We tested slightly different arrangements of the turn insulation and spacer materials in between the conductors. All withstood the cyclic load without major cracking. Some limited cracking was observed in the corners, as expected from the analysis. A photograph of the last two arrays tested is in Fig. 11. The difference between the arrays is in alignment: perfect alignment of the conductors versus slightly staggered one (in the foreground). Qualification of the turn insulation by testing is the only way to ensure the winding pack will operate reliably, when the design cannot be qualified by analysis.

The other valuable data we received from these tests is the elastic modulus and CTE of the winding pack. These data are necessary for design of the compression structure of the CS stack.

Fig. 11. Fatigue properties of the JK2LB jacket for CS conductor at 4 K and R=0.1

B. *Permeability of the epoxy through the glass under compression*

The CSM weight is more than 100 t, and the layers of glass at the bottom experience about 1.2 bar pressure. The amount of epoxy in the module is about 2,400 l, and it is important that the glass would have enough conductance to guarantee permeation into the whole volume of the CSM.

We performed a study of the epoxy permeation into the compressed glass [14, 15] and selected the glass cloths that had adequate strength and permeability. One type, 7781, satin weave, is a stronger glass, but with a limited permeability due to a higher glass content. The other type, 7500, is somewhat weaker, but with a better permeability due to plain weave construction that gives a slightly lower glass density per unit volume.

C. *Insulation of the special parts*

The CSMC has several areas where ground insulation requires very careful attention: (1) corners, where the vertical insulation interfaces with the horizontal insulation; (2) helium inlets and outlets; (3) breakouts from the CSM, where the conductor leaves the winding pack, bends, and runs vertically to the module terminations; and (4) penetration of the ground insulation by high voltage QD wires. All of these special parts, except the breakouts, were qualified by building a relevant mockup with the following high potential testing after a minimum of three thermal cycles between the room temperature and 80 K in the LN2 bath. Our prime contractor, GA, will qualify insulation of the breakout region soon.

D. *Mechanical properties of the insulating materials*

We qualified two types of glass cloth [16]—one with a higher strength and the other with a higher permeability—to be used in the ground insulation and between the pancakes in the CSM. We qualified two types of glass tape from the Carolina Narrow Fabric company for the turn insulation in our 4 × 4 tests with a satin weave (1581) and a plain weave (75712) construction. We measured dielectric and shear strength of ground insulation [17] and turn insulation at different conditions. We verified the shear strength of the turn insulation with grit blasting before and after heat treatment and substantiated grit blasting operation before HT as an acceptable process.

E. *Vacuum Pressure Impregnation process development and qualification*

The VPI process was established successfully during the CSMC fabrication [18]. The process involved a long pumping on the dry coil under the vacuum at elevated temperatures to remove most of the water retained by the glass, injecting the resin into the mold slowly under vacuum to eliminate any voids, applying several pressure-vacuum cycles and then gelling it under pressure, raising temperature and curing the resin at the prescribed temperature for a certain duration, and finally cooling slowly and uniformly to avoid cracking and high thermal stresses. However, the insulation design in the CSMC was quite different, allowing much easier resin permeation; therefore, we had to verify that this method would work with the new insulation design. To demonstrate the VPI process, we built a full cross section of the CSM but only 0.5 m long. Bars imitating the conductors were insulated with the designed turn insulation, and the glass build between the conductors was representative of the CSM design. We used silicone putty to prevent the resin from entering the ends of the bars, simulating the condition of the CSM in the mold.

The 14 × 40 array is shown in Fig. 12 after impregnation. There were several concerns about impregnation. One was to see if the staggered holes in the otherwise impermeable kapton sheets in the horizontal ground insulation are sufficient for adequate resin flow. Another concern was about design of the vertical ground insulation and whether it had a good permeation by the resin (there was a narrow gap 2 m long for the resin to travel in between two impermeable surfaces). Although parts of the design issues were verified on the mockups, the integrated test of 14 × 40 was a crucial demonstration [19]. In this project, we also studied outgassing during evacuation, drying of the winding pack in insulation before injection, and pressure drop across the winding pack. The array was heavily instrumented by thermocouples to see heat transfer between the surface and the middle of the winding pack during warm up, resin injection, gelling, curing, and cool down of the pack.

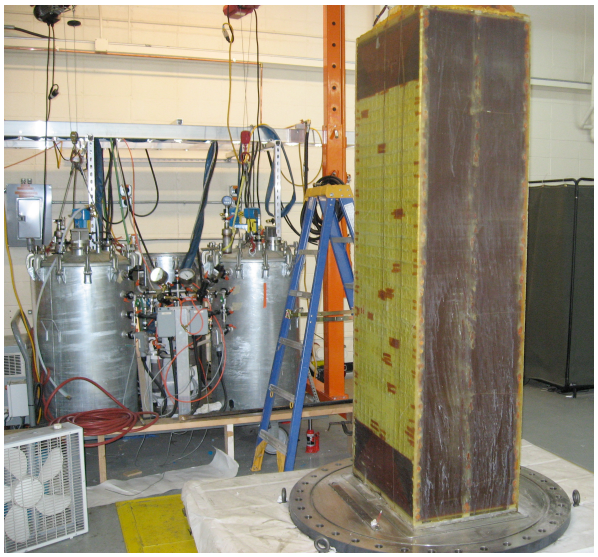

Fig. 12. A 14 × 40 array after VPI. Resin mixing tanks are seen in the background

Overall, we gained a valuable experience with this 14 × 40 project. After completion of the VPI, we de-sectioned the array in many cross sections and looked for defects in the array. We did not see any voids; the permeation was very good in all the inspected cross sections.

Overall, the project was successful; we obtained a confirmation to the developed design, procedure, drying, injection, filling rate, and amount of epoxy required for the complete fill of the CSM.

We also discovered a somewhat unexpected phenomenon. After removing the mold, we observed that the winding pack reduced the height by 20–25 mm, with the reduction more in the middle of the pack, less at the periphery.

The reasons of such a shrinkage were not immediately obvious, but several hypotheses were considered: (1) compressive creep of dry glass under the dead weight load; (2) creep of the wet glass, or lubrication of the glass by the epoxy resin that made the glass yarn move relative to each other; (3)

shrinkage of the epoxy during gelling and curing because of development of cross links; and, (4) elevated temperature for gelling, which caused glass–epoxy system movement and some other changes. We studied the literature and contacted experts in the field of VPI but did not discover any significant studies on the subject, mostly because impregnation of high objects with such a high dead weight load is rare. Although some small shrinkage after VPI was reported in the toroidal field model coil project [20], it was not a well-known and understood phenomenon. Because the tolerances on the winding pack height are ±2 mm, we performed a dedicated study on the subject to understand its nature and develop mitigation [21].

We built several mockups with a representative number of insulated conductors (7–12) and studied displacement of the pack under vertical compaction at different stages of VPI operation.

A principle of the studies (Fig. 13) shows a column of conductors under controlled pressure applied by a spring loaded mechanism (or pneumatic actuators) and monitored height of the stack with a displacement sensor.

Fig. 13. Cross section of the 12 × 1 array used for the winding pack height management study during assembly and VPI.

Main results of the study are given in [21]. Most of the compression of the winding pack takes place at the dry glass stage. The glass compaction is plastic–elastic—it has some irreversible compaction but also some springback. It is reproducible and can be learned to become predictable. Displacement during injection of the resin, warming up to the gelling temperature, gelling, then bringing to the curing temperature, curing, and cooling down all give some detectable displacement, but significantly less than the compaction of the dry glass. To obtain accurately controlled height of the winding pack, it is necessary to compact the glass during pack assembly, preferably multiple times because the stack is assembled for more accurate control. Also, it is necessary to keep applied pressure on the winding pack in the mold after the mold is closed and during resin injection and gelling. GA will optimize the equipment and the procedure of the production VPI with lessons learned to produce a tight tolerance winding pack during qualification efforts on the VPI station and the full diameter mockup coil. That will qualify the procedure for production modules fabrication.

IX. Characterization of Materials for ITER Central Solenoid

The ITER CS project required characterization of many materials that were not characterized in previous projects. A few examples are given below.

A. *Extension of the epoxy resin pot life*

The VPI process will require a record amount of epoxy transferred in the mold. Taking into account a very slow process of resin transfer to avoid formation of voids in the winding pack and the ground insulation, a pot life of resin (time before mixing and setting) may be desirable to extend. We carried out a study on extension of the pot life of resin without jeopardizing mechanical properties and discovered that this is possible by varying the amount of the accelerator in the three-component resin [22].

B. *Characterization of the jacket base material and welds*

The jacket material of the CS conductor, high manganese stainless steel, was selected because of the low coefficient of thermal expansion, high fracture toughness, and low crack growth propagation. The jacket is the main structural element of the CSM, and it experiences high stresses in high cycle loading conditions that are required of the CSM. Characterization of the base metal and the welds was necessary for assessment of the safety margin and jacket life in ITER operation.

Fig. 14 shows fatigue stress-cycles characterization of the jacket material and the welds as an example. Physical properties, CTE impact resistance, fracture toughness, and crack growth propagation parameters all were measured at 4 K [23, 24].

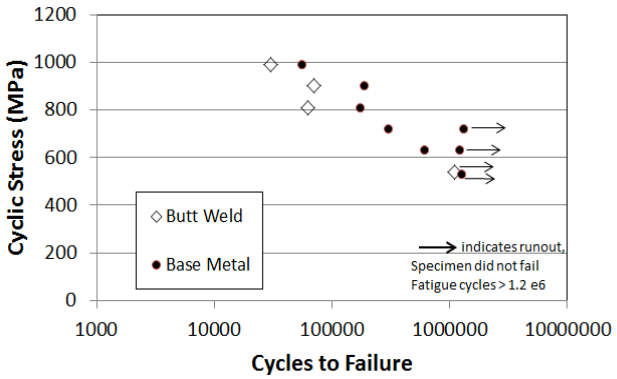

Fig. 14. Fatigue properties of the JK2LB jacket for the CS conductor at 4 K and R = 0.1.

Conclusions

The CSM R&D program is the most comprehensive development effort on magnets of this type. It required involvement of more than 20 organizations over 6 years and

provided the necessary basis of information for construction of the ITER CSM.

REFERENCES

[1] N. Martovetsky, P. Michael, J. Minervini, A. Radovinsky, et al., "ITER CS model coil and CS insert test results," IEEE Transactions on Applied Superconductivity, vol. 11, no. 1, pp. 2030–2033, March 2001.

[2] N. N. Martovetsky, A. B. Berryhill, and S. J. Kenney, "Qualification of the joints for the ITER Central Solenoid," IEEE Transactions on Applied Superconductivity, vol. 11, no. 3, p. 4804004, June 2012.

[3] A. Ulbricht, J. L. Duchateau, W. H. Fietz, et al., "The ITER toroidal field model coil project," Fusion Engineering and Design, vol. 73, issues 2–4, pp. 189–327, October 31, 2005.

[4] N. N. Martovetsky, S. J. Kenney, and J. R. Miller, "Development of the joints for ITER Central Solenoid," IEEE Transactions on Applied Superconductivity, vol. 21, no. 3, pp. 1922–1925, June 2011.

[5] R. L. Myatt, N. N. Martovetsky, C. Barbier, and K. D. Freudenberg, "ITER CS conductor helium inlet design optimization and evaluation," Fusion Science and Technology, vol. 64, no. 2, pp. 161–167, August 2013.

[6] R. Zanino, N. N. Martovetsky, A. Pasquali, L. Savoldi-Richard, and D. Speziani, "Computational thermal-hydraulic analysis of the helium inlet options for the ITER Central Solenoid," IEEE Transactions on Applied Superconductivity, vol. 22, no. 3, p. 4902505, June 2012.

[7] Y. Kudryavtsev and J. Kleiman, "Increasing fatigue strength of welded joints by ultrasonic impact treatment," International Institute of Welding Document XIII-2338-10, Structural Integrity Technologies Inc., Markham Ontario, Canada, 2010.

[8] N. N. Martovetsky and A. L. Radovinsky, "ITER CS quench detection system and its qualification by numerical modeling," IEEE Transactions on Applied Superconductivity, vol. 24, no. 3, p. 4202104, June 2014.

[9] N. N. Martovetsky, T. L. Mann, J. R. Miller; R. P. Reed, R. P. Walsh, J. D. McColskey, and D. Evans, "ITER central solenoid coil insulation qualification," Advances in Cryogenic Engineering Materials, vol. 56, pp. 135–144, 2010

[10] R. P. Reed, R. P. Walsh, T. Weeks, J. D. McColskey, and N. N. Martovetsky, "Compression-fatigue, elastic modulus, and thermal contraction of insulated conduit arrays of ITER CS modules," IEEE Transactions on Applied Superconductivity, vol. 23, issue 3, part 2, p. 4200805, 2013.

[11] R.P. Reed, "Large-scale fatigue tests and thermal contraction of two 4 × 4 insulated conduit arrays—Part I, preparation," US ITER US_D_2337HE, vol. 1.0, 2014.

[12] R. P. Reed, "Large-scale fatigue tests and thermal contraction of two 4 × 4 insulated conduit arrays—Part II, sample preparation and NIST test results," US ITER, US_D_235YXV, vol. 1.0, 2014.

[13] R. P. Reed, "Large-scale fatigue tests and thermal contraction of two 4 × 4 insulated conduit arrays—Part III, final," US ITER US_D_23BQ3Q, vol. 1.0, 2014.

[14] R. P. Reed, N. Martovetsky, J. Miller, T. Mann, F. Roundy, S. A., "Resin permeation through compressed glass insulation for U.S. ITER CS coil," Advances in Cryogenic Engineering Materials, vol. 56, pp. 111–118, 2010

[15] R. Reed, F. Roundy, and P. Biermann, "The flow of epoxy resin under compressive load through Holey kapton sheet and glass cloth (resin permeation studies)," US ITER US_22FJAB, October 2, 2013.

[16] R. P. Reed, M. Madhukar, B. Thaicharoenporn, and N. N. Martovetsky, "Low-temperature mechanical properties of glass/epoxy laminates," AIP Conference Proceedings, vol. 1574, no. 109, 2014. doi: 10.1063/1.4860612.

[17] R. P. Reed, R. P. Walsh, R. Duckworth, and I. Sauers, "Vacuum pressure impregnation (VPI) of 14 × 40 array of insulated conduit part III mechanical and electrical tests of ground insulation," US ITER US_22HQ4X, October 3, 2013.

[18] R. P. Reed, D. Evans, P. E. Fabian, "Development of a new resin system for the U.S. ITER Central Solenoid model coil," Advances in Cryogenic Engineering Materials, pp. 227–234, 2000.

[19] R. P. Reed, D. K. Irick, P. Biermann, F. Roundy, and N. N. Martovetsky, "Fabrication of an ITER CS module cross-section," Advances in Cryogenic Engineering Materials, vol. 60, pp. 146–153, 2014.

[20] R. Maix, H. Fillunger, et al., "Completion of the ITER toroidal field model coil (TFMC)," Fusion Engineering and Design, vol. 58–59, pp. 159–164, November 2001.

[21] N. N. Martovetsky, D. K. Irick, R. P. Reed, R. Haefelfinger, and E. Salazar, "Winding pack height management during fabrication of the ITER CS module," ICEC 25–ICMC 2014 Conference, Physics Procedia, , in press.

[22] M. S. Madhukar, and N. N. Martovetsky, "DGEBF epoxy blends for use in the resin impregnation of extremely large composite parts," Journal of Composite Materials, in press

[23] R. P. Walsh, K. Han, D. M. McRae, and N. N. Martovetsky, "Tensile and fatigue qualification testing of the ITER CS conduit alloy JK2LAB," presented at the ICMC 2014 Conference, University of Twente, Enschede, The Netherlands, July 2014.

[24] R. P. Walsh, K. Han, V. J. Toplosky, N. N. Martovetsky, T. L. Mann Jr., and J. R. Miller, "Mechanical properties of the modified JK2LB for Nb3Sn CICC applications," AIP Conference Proceedings, vol. 1219, pp. 17–24, 2010.